We are IntechOpen, the world's leading publisher of Open Access books Built by scientists, for scientists

4,800
Open access books available

122,000
International authors and editors

135M
Downloads

Our authors are among the

154
Countries delivered to

TOP 1%
most cited scientists

12.2%
Contributors from top 500 universities

CLARIVATE ANALYTICS BOOK CITATION INDEX INDEXED

WEB OF SCIENCE™

Selection of our books indexed in the Book Citation Index in Web of Science™ Core Collection (BKCI)

Interested in publishing with us?
Contact book.department@intechopen.com

Numbers displayed above are based on latest data collected.
For more information visit www.intechopen.com

9

Channel Assignment in Multihop Cellular Networks

Xue Jun Li and Peter Han Joo Chong
School of EEE, Nanyang Technological University
Singapore

1. Introduction

Recently, several work related to channel assignment for MCN-type systems were reported. Wu et al proposed diverting traffic from the congested cells to the non-congested cells (Wu et al., 2001; Wu et al., 2004), which is achieved by relaying traffic through unlicensed frequency band, such as the industrial, scientific and medical (ISM) band. For iCAR (Wu et al., 2001; Wu et al., 2004), ad hoc relay stations (ARSs), either being fixed (Wu et al., 2001) or mobile (Wu et al., 2004), are deployed for balancing traffic. The communication link between a mobile station (MS) and an ARS is established using the ISM band. Similarly, UCAN is used to increase the system throughput through relaying using the ISM band (Luo et al., 2003). None of the above papers describes how to select and allocate the relay channels for each hop in detail.

An ad hoc GSM (A-GSM) protocol was proposed in (Aggelou & Tafazolli, 2001) using the cellular frequency band for RSs to cover dead spots and increase the capacity. Aggelou and Tafazolli (Aggelou & Tafazolli, 2001) investigated the concept of A-GSM, which includes A-GSM network components, protocol architecture, and handover procedure to allow a MS to perform GSM-to-A-GSM and A-GSM-to-A-GSM handovers. The GSM-to-GSM connection uses the resource from the BS. The A-GSM-to-GSM connection routes through the RS and uses the resource from that RS. The coordinating of the allocation of resources of a relay node is controlled by a resource manager. However, it did not clearly address how the resources are allocated to the BS and RSs. It also did not address the channel assignment method for each type of connection. In addition, the analysis for a single GSM cell is done in (Aggelou & Tafazolli, 2001) so that the co-channel interference, which is one of the major issues in channel assignment in cellular networks, is not considered. Similarly, the MCN in (Hsu & Lin, 2002) assumes to use cellular frequency for relaying, whereas no clear description on how to allocate a channel to a MS for cellular or ad hoc mode is included.

2. Clustered multihop cellular networks

The key idea of CMCN (Li & Chong, 2006) is to achieve the characteristics of the macrocell/microcell hierarchically overlaid system (Rappaport & Hu, 1994; Yeung & Nanda, 1996) by applying the MANETs clustering (Yu & Chong, 2005) in *traditional* SCNs. In SCNs, the BS will cover the whole macrocell with a radius of r_M, as shown in Figure 1(a). The proposed CMCN divides the macrocell area into seven microcells with a radius of r_m in

order to increase the spectrum efficiency as shown in Figure 1(b). Six *virtual* microcells with a coverage radius of r_m around the central microcell will be formed as six clusters.

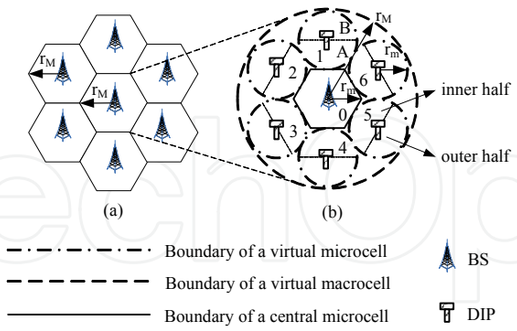

Fig. 1. (a) SCNs and (b) CMCN.

We proposed to use a DIP as a clusterhead in each *virtual* microcell for CMCN. A DIP is a wireless communication device, which has no wired interface. This is different from a BS, which may have a wired interface to a mobile switching center (MSC). Next, DIPs can be mobile and can be relocated anywhere to provide services while the locations of BSs are fixed due to the wired (or microwave) connection to MSC. The function of a DIP includes allocating channels to the MSs within its microcell, selecting a MS as a RS, and determining the routing path. Specially, DIPs can help the BS to perform the function of authentication, authorization and accounting (AAA). For example, a DIP is able to authorize a MS to relay the traffic for another MS. Different from ARSs in iCAR (Wu et al., 2001) or wireless ports in (Kudoh & Adachi, 2005) and (Liu et al., 2006), DIPs are not involved in data relaying. Hence, no worry about the capacity saturation problem, such as the load balancing considered in (Liu et al., 2006) for RSs, is concerned. Earlier researches have established that as long as there is a large number of MSs in the service area, it is not difficult for a DIP to find a RS. As a DIP only helps exchange the control/signaling information with a BS and MSs through the control channels, its complexity is much lower than a BS, so does the cost.

We assume that a DIP is installed in the center of a *virtual* microcell. The BS covers the central microcell and six DIPs cover the six *virtual* microcells. Each *virtual* microcell is divided into two regions: inner half and outer half. The inner half is near the central microcell. For example, as shown in Figure 1(b), for *virtual* microcell 1, area A is the inner half and area B is the outer half. This structure is named as *seven-cell* CMCN architecture.

In CMCN, BSs will have two levels of transmit power, P_{data} and $P_{control}$. As referred to Figure 1(b), P_{data} is used for a BS to transmit data packets including acknowledgement packets within its coverage area with a radius of r_m in the central microcell. P_{data} is also used for a MS to transmit data or control packets for a transmission range of radius, r_m. $P_{control}$ is used by the BS for transmitting the control/signaling packets between a BS and a DIP inside a *virtual* macrocell with a radius of r_M so that the BS is able to exchange the control/signaling information with every DIP.

3. Proposed fixed channel assignment scheme

In *traditional* SCNs, the channels assigned for uplink and downlink transmissions are balanced in every cell for symmetric traffic, such as voice calls. The number of channels assigned to the uplink and downlink for each call is the same. In practice, the FCA in SCNs

normally assigns the same number of channels for uplink and downlink transmissions in each cell. However, in CMCN, taking both uplink and downlink transmissions into consideration, the channel assignment for uplink and downlink transmissions of a call is unbalanced. Thus we propose an AFCA to assign different number of uplink and downlink channels in each cell to provide the optimal capacity.

For AFCA in CMCN, each central/*virtual* microcell is assigned a set of channels for the uplink and downlink according to the AFCA rules. As shown in Figure 2, the channel assignment to calls in CMCN can be implemented as follows:

1) One-Hop Calls: If a MS, MS_1, originates a new call from the central microcell, it will require one uplink channel and one downlink channel. If all the uplink channels in the central microcell are occupied, or all the downlink channels in the central microcell are occupied, that new call will be blocked. Thus, a one-hop call takes one uplink channel and one downlink channel from the central microcell.

2) Two-Hop Calls: If a MS, MS_2, originates a new call from the inner half of the i^{th} *virtual* microcell, for uplink transmission, it will request an uplink channel belonging to the i^{th} *virtual* microcell from its DIP. Since the DIP is assigned a set of channels for use in its microcell, it will know the availability of channel within its *virtual* microcell to assign a free channel to that MS, MS_2. Then, the DIP will help find a MS, RS_0, in the central microcell as a RS, which will request another uplink channel belonging to the central microcell for relaying the call to BS. Thus, that new two-hop call will occupy one uplink channel from the i^{th} *virtual* microcell and one uplink channel from the central microcell for uplink transmission. For downlink transmission, it requires two downlink channels from the central microcell, one for the BS to the RS, RS_0, and the other for RS_0 to the MS, MS_2. Therefore, as shown in Figure 2, a two-hop call, originated by MS_2, requires one uplink channel belonging to the central microcell and one uplink channel belonging to the i^{th} *virtual* microcell, and two downlink channels belonging to the central microcell. That is why the channel assignment to the uplink and downlink is unbalanced in each *virtual* or central microcell. A new call will be blocked if either of the following conditions comes into existence: (i) there is no free uplink channel in the i^{th} *virtual* microcell; (ii) there is no free uplink channel in the central microcell; (iii) there are less than two free downlink channels in the central microcell. When the call is completed, the MS, MS_2, in the *virtual* microcell will inform its DIP to release the channels for its call. Then, the DIP can update the channel status accordingly.

3) Three-Hop Calls: If a MS, MS_3, originates a new call from the outer half of the i^{th} *virtual* microcell, for uplink transmission, it will require two uplink channels belonging to the i^{th} *virtual* microcell from the DIP. This is because it takes two hops to reach the central microcell, as shown in Figure 2. Then, it will request one more uplink channel belonging to central microcell for a relay MS in the central microcell. For downlink transmission, it will require two downlink channels from the central microcell—one for the BS to the RS in the central microcell and the other for the RS in the central microcell to the RS in the i^{th} *virtual* microcell. It will require one more downlink channel from i^{th} *virtual* microcell, for the downlink transmission from the RS in the i^{th} *virtual* microcell to the MS. As shown in Figure 2, a three-hop call, originated by MS_3, requires two uplink channels in the i^{th} *virtual* microcell and one uplink channel in the central microcell, and one downlink channel from the i^{th} *virtual* microcell and two downlink channels from the central microcell. A call will be blocked if either of the following conditions fails: (i) there is at least one free uplink channel in the central microcell; (ii) there at least two free uplink channels in the i^{th} *virtual* microcell; (iii) there are at least two free downlink channels in the central microcell; (4) there is at least

one free downlink channel in the i^{th} *virtual* microcell. Similarly, when the call is completed, the MS, MS_3, in the *virtual* microcell will inform its DIP to release the channels for its call. Then, the DIP can update the channel status accordingly.

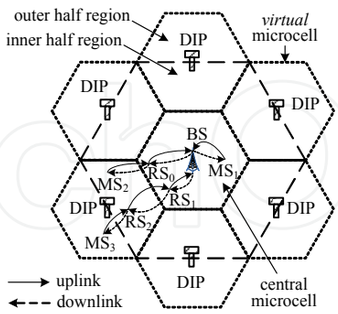

Fig. 2. Channel assignment for different types of calls.

In *traditional* SCNs as shown in Figure 1(a), if there are 70 uplink/downlink channels in the system, under the uniform FCA with a reuse factor of 7, each macrocell will be assigned 10 uplink/downlink channels. However, in our proposed CMCN architecture, as shown in Figure 1(b), each macrocell is split into one central microcell and six *virtual* microcells. Under the AFCA for CMCN, each (*virtual* or central) microcell is assigned N_U uplink and N_D downlink channels, whereas the FCA in SCNs allocates the same number of channels for the uplink and downlink. For inter-macrocell traffic of MCN (Hsu & Lin, 2002), as the BS in the central microcell is involved in all the calls including its own microcell and the surrounding six *virtual* microcells, more channels should be assigned to the central microcell in order to reduce the call blocking probability. If X_U uplink and X_D downlink channels are taken from each of the six surrounding *virtual* microcells, $6X_U$ uplink and $6X_D$ downlink channels can be added to the central microcell. The optimum uplink and downlink channel assignment to the system will be studied later.

3.1 Analytical models

To analyze the AFCA scheme in CMCN, we first study a hypothetical two-cell CMCN. Based on the methodology developed for the two-cell CMCN, we analyze the proposed AFCA scheme for the seven-cell CMCN. To make the problem tractable, we have assumed low mobility such that no handover or channel reassignment is required. Next, we have considered that it takes at most three hops for a MS to reach the BS. And the transmission range of a MS for each hop is the same.

In our analysis, we are considering a TDMA cellular system, in which the uplink and downlink channels are separated by half of the total allocated bandwidth. In traditional cellular systems, the uplink channel assignment and downlink channel assignment are symmetric. Thus, if the uplink is blocked, then the downlink is also blocked due to the symmetry between the uplink and the downlink channel assignment and symmetric uplink and downlink bandwidth allocation. Researchers usually study the channel assignment regardless of uplink and downlink in the literature. However, channel assignment in CMCN is different from that in *traditional* cellular systems that the uplink and downlink channel assignments are not symmetric. Specifically, for multihop calls, the downlink channel assignment requires more channels than the uplink channel assignment in the central microcells in CMCN. In addition, since uplink channel assignment and downlink channel

assignment are independent in CMCN, the uplink blocking is independent of the downlink blocking. Hence, we are able to analyze the uplink and downlink performance separately. In fact, the uplink/downlink channel assignment does not imply the downlink/uplink channel available. On the contrary, a call is blocked if either uplink or downlink channel assignment is unsuccessful. Therefore, we have to consider the channel assignment for uplink and downlink transmission separately in order to study the distinct feature of CMCN. Otherwise, we are not able to find whether the call blocking is due to lack of uplink channels or it is due to lack of downlink channels.

3.2 Analytical models for uplink

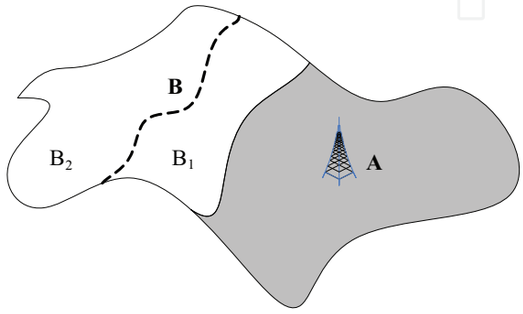

Fig. 3. A hypothetical two-cell CMCN.

We consider a hypothetical two-cell CMCN with the assumption that cell A and cell B have the same area. As shown in Figure 3, cell B is equally divided into two regions, B_1 and B_2. N_0 uplink channels and N_1 uplink channels are assigned to cell A and cell B, respectively. For uplink transmission, upon a call arrival in cell A, one channel will be assigned to the call, if any; otherwise, the call is blocked. This type of call is considered as one-hop call. Call arrivals in the sub-cell B_1 are considered as two-hop calls and call arrivals in sub-cell B_2 are considered as three-hop calls. For a two-hop call arrival, if there is at least one channel available in cell A and at least one channel available in cell B, then the call is accepted and two channels are assigned to the link, one from the cell A and one from the cell B; otherwise, the two-hop call is blocked. Similarly, when a three-hop call arrives, if there is at least one channel available in cell A and at least two channels available in cell B, the call is accepted; otherwise, the three-hop call is blocked.

The proposed AFCA scheme with a hypothetical two-cell CMCN for uplink transmission can be modeled by a three-dimensional Markov chain. For example, if N_0=4 and N_1=4, the Markov chain is shown in Figure 4. All the states form a set Π, which is given by

$$\Pi = \left\{(x,y,z) \mid 0 \le x \le N_0, 0 \le y \le N_1, 0 \le z \le \lfloor N_1 / 2 \rfloor, x + y + z \le N_0, y + 2z \le N_1\right\} \tag{1}$$

where x, y and z stands for the number of one-hop, two-hop and three-hop calls, respectively. λ is the total call arrival rate. With uniform call arrivals, the call arrival rates are $\lambda_1 = \lambda/2$, $\lambda_2 = \lambda/4$ and $\lambda_3 = \lambda/4$ for one-hop, two-hop and three-hop calls, respectively. The corresponding service rates for three types of calls from state (x, y, z) are

$$\mu_1(x,y,z) = x\mu,\ \mu_2(x,y,z) = y\mu,\ \mu_3(x,y,z) = z\mu \tag{2}$$

where λ_i and $\mu_i(x, y, z)$ are the arrival rate and the service rate for i-hop calls, respectively. Thus, $\rho=\lambda/\mu$ gives the offered traffic per two-cell CMCN in Erlangs. Due to the limited space, we simply use μ_j to represent $\mu_j(x, y, z)$ in Figure 4, where j=1, 2 or 3.
By applying the global balance theory (Kleinrock, 1975), we can obtain a global-balance equation for each state in Π. For example, for state (1, 0, 1) in Figure 4, we have

$$\begin{aligned} &P(1,0,1)\times[\lambda_1+\lambda_2+\lambda_3+\mu_1(1,0,1)+0+\mu_3(1,0,1)]= \\ &P(0,0,1)\times\lambda_1+0\times\lambda_2+P(1,0,0)\times\lambda_3+ \\ &P(2,0,1)\times\mu_1(2,0,1)+P(1,1,1)\times\mu_2(1,1,1)+P(1,0,2)\times\mu_3(1,0,2) \end{aligned} \tag{3}$$

where $P(x, y, z)$ is the probability of state (x, y, z). Then we have

$$\begin{aligned} &P(1,0,1)\times[\lambda_1+\lambda_2+\lambda_3+\mu_1(1,0,1)+0+\mu_3(1,0,1)]- \\ &P(0,0,1)\times\lambda_1-0\times\lambda_2-P(1,0,0)\times\lambda_3- \\ &P(2,0,1)\times\mu_1(2,0,1)-P(1,1,1)\times\mu_2(1,1,1)-P(1,0,2)\times\mu_3(1,0,2)=0 \end{aligned} \tag{4}$$

The total state probability sums to unity, i.e.,

$$\sum_{(x,y,z)\in\Pi} P(x,y,z)=1 \tag{5}$$

For a set Π with m states, the array of global-balance equations can be transformed as

$$[A]_{m\times m}[P]_{m\times 1}=[B]_{m\times 1} \tag{6}$$

$$[A]=\begin{bmatrix} 1 & 1 & \cdots & 1 \\ t_{21} & t_{22} & \cdots & t_{2m} \\ \vdots & \vdots & \cdots & \vdots \\ \vdots & \vdots & t_{ii} & \vdots \\ \vdots & \vdots & \cdots & \vdots \\ t_{m1} & t_{m2} & \cdots & t_{mm} \end{bmatrix},\ [P]=\begin{bmatrix} P(x_1,y_1,z_1) \\ P(x_2,y_2,z_2) \\ \vdots \\ P(x_i,y_i,z_i) \\ \vdots \\ P(x_m,y_m,z_m) \end{bmatrix},\ [B]=\begin{bmatrix} 1 \\ 0 \\ \vdots \\ 0 \end{bmatrix} \tag{7}$$

Note that the states in Π are indexed, state i corresponds to (x_i, y_i, z_i). In matrix $[A]$, there are two types of transition rates:

- *Transition Rates into a State*: The element t_{ij} (when $i \neq j$) is the negative of the transition rate from state j to state i. For state j, we have

$$t_{ij}=\begin{cases} -\mu x_j, \text{ if } x_j-x_i=1; & -\lambda_1, \text{ if } x_j-x_i=-1; \\ -\mu y_j, \text{ if } y_j-y_i=1; & -\lambda_2, \text{ if } y_j-y_i=-1; \\ -\mu z_j, \text{ if } z_j-z_i=1; & -\lambda_3, \text{ if } z_j-z_i=-1; \\ 0, \text{ otherwise.} \end{cases} \tag{8}$$

- *Transition Rates out of a State*: The element t_{ii} is equal to the sum of the transition rates out of the state i. For state i, we have

$$t_{ii}=-\sum_{j=1,j\neq i}^{m} t_{ji} \tag{9}$$

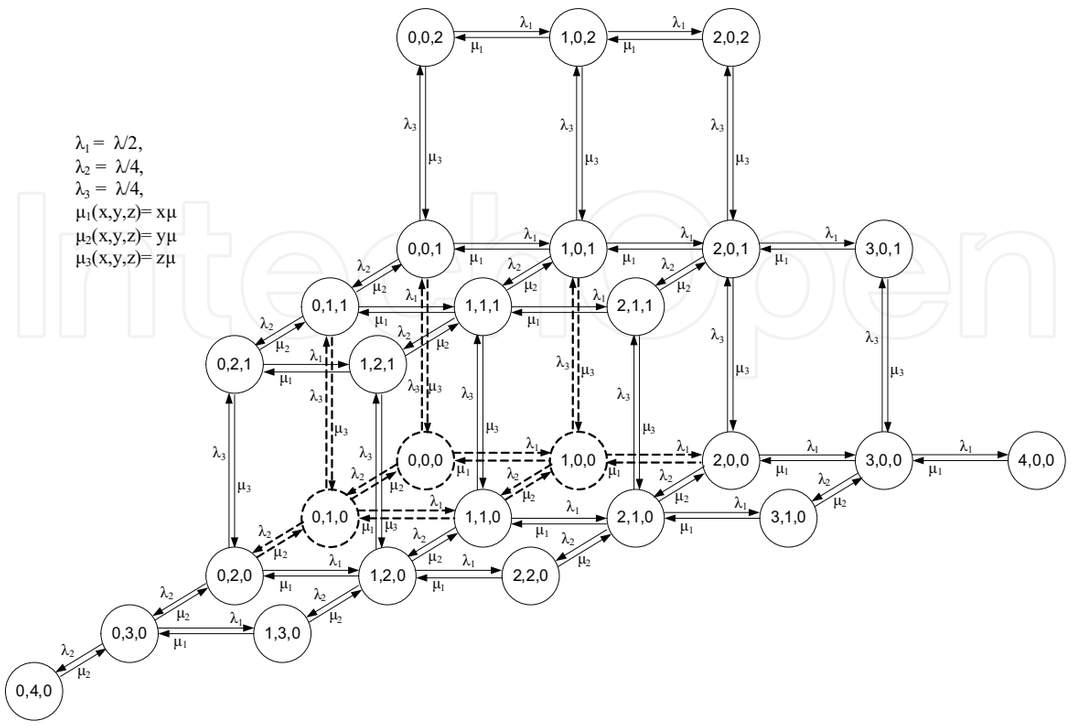

Fig. 4. Uplink exact model for the two-cell CMCN with N_0=4 and N_1=4.

By solving the matrix equation, we can get the matrix [P], which includes the probability for each state in Π. Denote P_{bi} as the average call blocking probability of i^{th}-hop calls, which is defined as the ratio of the number of blocked i^{th}-hop calls and the total number of call arrivals for i^{th}-hop calls over the whole *virtual* macrocell area. Then, we have

$$P_{b1} = \sum_{x=0}^{N_0} \sum_{y=0}^{N_1} \sum_{z=0}^{\lfloor N_1/2 \rfloor} P(x,y,z)\big|_{(x,y,z)\in\Pi, x+y+z=N_0} \tag{10}$$

$$P_{b2} = P_{b1} + \sum_{x=0}^{N_0} \sum_{y=0}^{N_1} \sum_{z=0}^{\lfloor N_1/2 \rfloor} P(x,y,z)\big|_{(x,y,z)\in\Pi,\ y+2z=N_1} + \sum_{x=0}^{N_0} \sum_{y=0}^{N_1} \sum_{z=0}^{\lfloor N_1/2 \rfloor} P(x,y,z)\big|_{(x,y,z)\in\Pi,\ x+y+z=N_0,\ \text{and}\ y+2z=N_1} \tag{11}$$

$$P_{b3} = P_{b1} + \sum_{x=0}^{N_0} \sum_{y=0}^{N_1} \sum_{z=0}^{\lfloor N_1/2 \rfloor} P(x,y,z)\big|_{(x,y,z)\in\Pi,\ y+2z\geq N_1-1} - \sum_{x=0}^{N_0} \sum_{y=0}^{N_1} \sum_{z=0}^{\lfloor N_1/2 \rfloor} P(x,y,z)\big|_{(x,y,z)\in\Pi,\ x+y+z=N_0,\ \text{and}\ y+2z\geq N_1-1} \tag{12}$$

Finally, the average uplink blocking probability of the system is given by

$$P_{b,U} = P_{b1} \times \lambda_1/\lambda + P_{b2} \times \lambda_2/\lambda + P_{b3} \times \lambda_3/\lambda \ . \tag{13}$$

The seven-cell CMCN model shown in Figure 1(b) is used to analyze the performance of the proposed AFCA scheme. For simplicity, we assume a reuse factor of N_r=7 in the analysis. The methodology can be applied for other N_r values. Thus, each macrocell area is divided

into N_r microcells. The channel assignment procedures will be different and the multi-dimensional Markov chain needs to be reconstructed.

Three types of new calls are originated from the system. They are calls originated from the central microcell, inner-half and outer-half *virtual* microcell as one-hop, two-hop and three-hop calls, respectively. With uniform call arrivals, we have $\lambda_1 = \lambda/7$, $\lambda_2 = 3\lambda/7$, $\lambda_3 = 3\lambda/7$; where λ_1, λ_2 and λ_3 are the call arrival rates for one-hop, two-hop and three-hop calls, respectively. And λ is the call arrival rate to a macrocell as shown in Figure 1(b). Hence the offered traffic load is $\rho_1 = \lambda_1/\mu$, $\rho_2 = \lambda_2/\mu$ and $\rho_3 = \lambda_3/\mu$ for one-hop, two-hop and three-hop calls, respectively. $1/\mu$ is average call duration. The offered traffic load per macrocell is given by $\rho = \lambda/\mu$.

For the seven-cell CMCN, the AFCA scheme can be modeled using a 13-dimensional Markov chain. The central microcell is assigned with N_0 channels and each of the six surrounding *virtual* microcells is assigned with N_1 channels. As shown in Figure 1(b), the seven microcell is numbered with 0, 1, 2, …, 6, starting from the central microcell. A state is defined as $(n_0^1, n_1^2, n_1^3, n_2^2, n_2^3, n_3^2, n_3^3, n_4^2, n_4^3, n_5^2, n_5^3, n_6^2, n_6^3)$. To make the analysis convenient, each state is numbered with an integer index s, and all the states form a set Π. For example, a state s corresponds to a distinct sequence of nonnegative integers $(n_0^1(s), n_1^2(s), n_1^3(s), n_2^2(s), n_2^3(s), n_3^2(s), n_3^3(s), n_4^2(s), n_4^3(s), n_5^2(s), n_5^3(s), n_6^2(s), n_6^3(s))$ where $n_i^j(s)$ is number of j-hop calls in microcell i at state s. The permissible states must satisfy the following constraints:

$$\begin{cases} n_0^1(s) + n_1^2(s) + n_1^3(s) + n_2^2(s) + n_2^3(s) + n_3^2(s) + n_3^3(s) \\ + n_4^2(s) + n_4^3(s) + n_5^2(s) + n_5^3(s) + n_6^2(s) + n_6^3(s) \le N_0 \\ 0 \le n_0^1(s) \le N_0; \quad 0 \le n_i^2(s) + 2n_i^3(s) \le N_1, \text{ for } i = 1,2,\cdots,6 \\ 0 \le n_i^2(s) \le N_1; \quad 0 \le n_i^3(s) \le \lfloor N_1/2 \rfloor, \text{ for } i = 1,2,\cdots,6 \end{cases} \tag{14}$$

A state transition can be caused by one of the following six events: an arrival of one-hop, two-hop or three-hop call; a departure of one-hop, two-hop or three-hop call. There are maximally 26 possible transitions for a state in the Markov chain model for seven-cell CMCNs. By comparing the state number of two states, we can obtain the transition rates. Applying the global-balance theory (Kleinrock, 1975), we can obtain one equation for each state. For example, as shown in Figure 5, for a state s_1 we may have,

$$\begin{aligned} &P(s_1)[\lambda_1 + \lambda_2/6 + \lambda_3/6 + \mu_1(s_1) + \mu_2(s_1) + \mu_3(s_1)] = P(s_2)\lambda_1 \\ &+P(s_3)\lambda_2/6 + P(s_4)\lambda_3/6 + P(s_5)\mu_1(s_5) + P(s_6)\mu_2(s_6) + P(s_7)\mu_3(s_7) \end{aligned} \tag{15}$$

where $P(s_i)$ is the steady-state probability of state s_i, and $\mu_j(s_i)$ is the service rate for j-hop calls at state s_i. Similarly, the total state probability sums to unity,

$$\sum_{s \in \Pi} P(s) = 1 \tag{16}$$

Again for a state set Π with m states, the array of global-balance equations form

$$[A]_{m \times m} [P]_{m \times 1} = [B]_{m \times 1} \tag{17}$$

$$[A]=\begin{bmatrix} 1 & 1 & \cdots & 1 \\ t_{21} & t_{22} & \cdots & t_{2m} \\ \vdots & \vdots & \cdots & \vdots \\ \vdots & \vdots & t_{ii} & \vdots \\ \vdots & \vdots & \cdots & \vdots \\ t_{m1} & t_{m2} & \cdots & t_{mm} \end{bmatrix},\ [P]=\begin{bmatrix} P(1) \\ P(2) \\ \vdots \\ P(i) \\ \vdots \\ P(m) \end{bmatrix},\ [B]=\begin{bmatrix} 1 \\ 0 \\ \vdots \\ 0 \end{bmatrix} \tag{18}$$

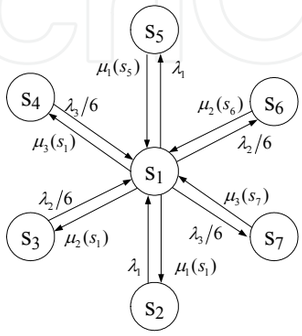

Fig. 5. Possible transitions for a state s_1.

In matrix [A], there are two types of transition rates:
Transition Rates into a State: The element t_{ij} (when $i \neq j$) is the negative of the transition rate from state j to state i. The service rates for the three types of calls in microcell (central or *virtual*) k from state j are respectively $\mu_1(j)=n_0^1(j)\mu$, $\mu_2(j)=n_k^2(j)\mu$, $\mu_3(j)=n_k^3(j)\mu$ where k=1, 2, …, 6. Therefore,

$$t_{ij}=\begin{cases} -n_0^1(j)\mu, \text{if } n_0^1(j)-n_0^1(i)=1; & -\lambda_1, \text{if } n_0^1(j)-n_0^1(i)=-1; \\ -n_k^2(j)\mu, \text{if } n_k^2(j)-n_k^2(i)=1; & -\lambda_2/6, \text{if } n_k^2(j)-n_k^2(i)=-1; \\ -n_k^3(j)\mu, \text{if } n_k^3(j)-n_k^3(i)=1; & -\lambda_3/6, \text{if } n_k^3(j)-n_k^3(i)=-1; \\ 0, \text{otherwise.} \end{cases} \tag{19}$$

Transition Rates out of a State: The element t_{ii} is equal to the sum of the transition rates out of state i. For state i, we have,

$$t_{ii}=-\sum_{j=1,j\neq i}^{m} t_{ji} \tag{20}$$

By solving the matrix equation, we can get the matrix [P]. Then, the blocking probabilities, P_{b1}, P_{b2} and P_{b3} for one-hop call, two-hop call and three-hop call in each cell is given by, respectively,

$$P_{b1}=\sum_{s\in\Pi} P(s)\Big|_{n_0^1(s)+\sum_{i=1}^{6}[n_i^2(s)+n_i^3(s)]=N_0} \tag{21}$$

$$P_{b2}=P_{b1}+\frac{1}{6}\sum_{i=1}^{6}\sum_{s\in\Pi} P(s)\Big|_{n_i^2(s)+2n_i^3(s)=N_1} -\frac{1}{6}\sum_{i=1}^{6}\sum_{s\in\Pi} P(s)\Big|_{n_i^2(s)+2n_i^3(s)=N_1 \text{ and } n_0^1(s)+\sum_{k=1}^{6}\left[n_k^2(s)+n_k^3(s)\right]=N_0} \tag{22}$$

$$P_{b3} = P_{b1} + \frac{1}{6}\sum_{i=1}^{6}\sum_{s\in\Pi} P(s)\Big|_{n_i^2(s)+2n_i^3(s)\geq N_1-1} - \frac{1}{6}\sum_{i=1}^{6}\sum_{s\in\Pi} P(s)\Big|_{n_i^2(s)+2n_i^3(s)\geq N_1-1 \text{ and } n_0^1(s)+\sum_{k=1}^{6}\left\lfloor n_k^2(s)+n_k^3(s)\right\rfloor=N_0} \quad (23)$$

Then, the average call blocking probability, $P_{b,U}$, is given by (13).

The exact model may result in excessive long computational time, especially for large N_0 and N_1. To reduce the computational load, we find an approximated model with much fewer states to analyze the AFCA scheme and the detailed analysis is available in (Li & Chong, 2010).

3.2.1 Analytical models for downlink

To analyze the AFCA scheme in CMCN with downlink transmission, again we first study the hypothetical two-cell CMCN model. After that, we analyze the proposed AFCA scheme for seven-cell CMCN model based on the methodology developed for the hypothetical two-cell CMCN model.

We consider the two-cell CMCN as shown in Figure 3. The BS is located in cell A, which has the same area with cell B, the *virtual* microcell. Cell B is equally divided into two regions, B_1 and B_2, and B_1 is next to cell A. N_0 downlink channels and N_1 downlink channels are assigned to cell A and cell B, respectively.

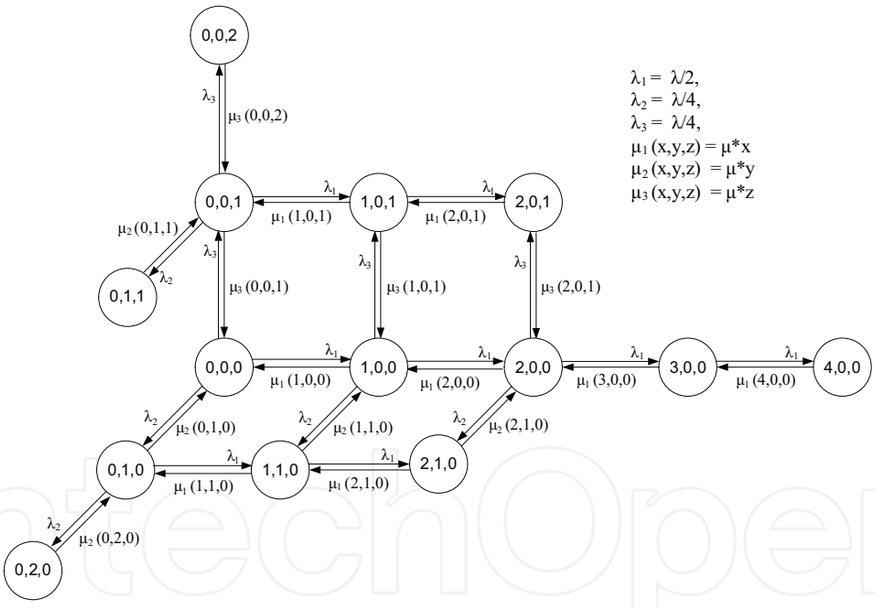

Fig. 6. Downlink exact model for the two-cell CMCN with N_0=4 and N_1=2.

For downlink transmission, a call arrival in cell A, considered as a one-hop call, will require one downlink channel, if any. Otherwise, the call is blocked. Call arrivals in the region B_1 are considered as two-hop calls, each of which takes two downlink channels from cell A. Call arrivals in region B_2 are considered as three-hop calls, each of which takes two downlink channels from cell A and one downlink channel from cell B. For a new two-hop call, if there are at least two downlink channels available in cell A, then the call is accepted; otherwise, the call is blocked. Similarly, when a three-hop call arrives, if there are at least two downlink channels available in cell A and at least one downlink channels available in cell B, the call is accepted. Otherwise, the call is blocked.

For downlink transmission, the AFCA scheme with the hypothetical two-cell CMCN can be modeled by a three-dimensional Markov chain. For example, if N_0=4 and N_1=2, the Markov chain can be drawn as Figure 6. All the states form a set Π,

$$\Pi = \{(x,y,z) \mid 0 \le x \le N_0, 0 \le y \le \lfloor N_0/2 \rfloor, 0 \le z \le N_1, x+2y+2z \le N_0\} \tag{24}$$

where x, y, z stands for the number of one-hop, two-hop and three-hop calls, respectively. With uniform call arrivals, the call arrival rates are $\lambda_1 = \lambda/2$, $\lambda_2 = \lambda/4$ and $\lambda_3 = \lambda/4$ for one-hop, two-hop and three-hop calls, respectively. λ is total call arrival rate to the two-cell CMCN. The corresponding service rates for three types of calls from state (x, y, z) are

$$\mu_1(x,y,z) = x\mu,\ \mu_2(x,y,z) = y\mu,\ \mu_3(x,y,z) = z\mu \tag{25}$$

where λ_i and $\mu_i(x, y, z)$ are the arrival rate and the service rate for i-hop calls, respectively. $1/\mu$ is the average call duration and $\rho = \lambda/\mu$ gives the offered traffic per two-cell CMCN in Erlangs.

Next, we apply the global balance theory (Kleinrock, 1975) and obtain a global-balance equation for each state in Π. For example, for state (1,0,0) in Figure 6, we have

$$\begin{aligned} &P(1,0,0)\times[\lambda_1+\lambda_2+\lambda_3+\mu_1(1,0,0)+0+0] = \\ &P(0,0,0)\times\lambda_1+0\times\lambda_2+0\times\lambda_3+P(2,0,0)\times\mu_1(2,0,0)+P(1,1,0)\times\mu_2(1,1,0)+P(1,0,1)\times\mu_3(1,0,1) \end{aligned} \tag{26}$$

where $P(x, y, z)$ is the probability of state (x, y, z). Then we have

$$\begin{aligned} &P(1,0,0)\times[\lambda_1+\lambda_2+\lambda_3+\mu_1(1,0,0)+0+0] \\ &-P(0,0,0)\times\lambda_1-0\times\lambda_2-0\times\lambda_3-P(2,0,0)\times\mu_1(2,0,0)-P(1,1,0)\times\mu_2(1,1,0)-P(1,0,1)\times\mu_3(1,0,1)=0 \end{aligned} \tag{27}$$

The total state probability sums to unity, i.e.,

$$\sum_{(x,y,z)\in\Pi} P(x,y,z) = 1 \tag{28}$$

For a state set Π having m states, the array of global-balance equations form

$$[A]_{m\times m}[P]_{m\times 1} = [B]_{m\times 1} \tag{29}$$

$$[A] = \begin{bmatrix} 1 & 1 & \cdots & 1 \\ t_{21} & t_{22} & \cdots & t_{2m} \\ \vdots & \vdots & \cdots & \vdots \\ \vdots & \vdots & t_{ii} & \vdots \\ \vdots & \vdots & \cdots & \vdots \\ t_{m1} & t_{m2} & \cdots & t_{mm} \end{bmatrix},\ [P] = \begin{bmatrix} P(x_1,y_1,z_1) \\ P(x_2,y_2,z_2) \\ \vdots \\ P(x_i,y_i,z_i) \\ \vdots \\ P(x_m,y_m,z_m) \end{bmatrix},\ [B] = \begin{bmatrix} 1 \\ 0 \\ \vdots \\ 0 \end{bmatrix} \tag{30}$$

Note that the states in Π are indexed, state s corresponds to (x_s, y_s, z_s). In matrix [A], there are two types of transition rates:

Transition Rates into a State: The element t_{ij} (when $i \neq j$) is the negative of the transition rate from state j to state i. For state j, we have

$$t_{ij} = \begin{cases} -\mu x_j, \text{ if } x_j - x_i = 1; & -\lambda_1, \text{ if } x_j - x_i = -1; \\ -\mu y_j, \text{ if } y_j - y_i = 1; & -\lambda_2, \text{ if } y_j - y_i = -1; \\ -\mu z_j, \text{ if } z_j - z_i = 1; & -\lambda_3, \text{ if } z_j - z_i = -1; \\ 0, \text{ otherwise.} \end{cases} \tag{31}$$

Transition Rates out of a State: The element t_{ii} is equal to the sum of the transition rates out of the state i. For state i, we may have

$$t_{ii} = -\sum_{j=1, j\neq i}^{m} t_{ji} \tag{32}$$

By solving the matrix equation, we can get the matrix [P], which includes the probability for each state in Π. Then, the blocking probability for one-hop, two-hop and three-hop calls can be calculated as follows:

$$P_{b1} = \sum_{x=0}^{N_0} \sum_{y=0}^{\lfloor N_0/2 \rfloor} \sum_{z=0}^{N_1} P(x,y,z)\big|_{(x,y,z)\in\Pi,\ x+2y+2z=N_0} \tag{33}$$

$$P_{b2} = \sum_{x=0}^{N_0} \sum_{y=0}^{\lfloor N_0/2 \rfloor} \sum_{z=0}^{N_1} P(x,y,z)\big|_{(x,y,z)\in\Pi,\ x+2y+2z\geq N_0-1} \tag{34}$$

$$P_{b3} = P_{b2} + \sum_{x=0}^{N_0} \sum_{y=0}^{\lfloor N_0/2 \rfloor} \sum_{z=0}^{N_1} P(x,y,z)\big|_{(x,y,z)\in\Pi,\ z=N_1} - \sum_{x=0}^{N_0} \sum_{y=0}^{\lfloor N_0/2 \rfloor} \sum_{z=0}^{N_1} P(x,y,z)\big|_{(x,y,z)\in\Pi,\ x+2y+2z\geq N_0-1,\ \text{and } z=N_1} \tag{35}$$

Finally, the average blocking probability, $P_{b,D}$, of the system for downlink is given by

$$P_{b,D} = P_{b1} \times \lambda_1/\lambda + P_{b2} \times \lambda_2/\lambda + P_{b3} \times \lambda_3/\lambda \tag{36}$$

The seven-cell CMCN model shown in Figure 1(b) is used to analyze the performance of the proposed AFCA scheme. For simplicity, again N_r=7 is used in the analysis. The methodology can be applied for other N_r. Thus, each macrocell area is divided into N_r microcells. The channel assignment procedures will be different and the multi-dimensional Markov chain needs to be reconstructed.

Three types of new calls are originated from the system. They are calls originated from the central, inner-half and outer-half microcell as one-hop, two-hop and three-hop calls, respectively. With uniform call arrivals, $\lambda_1 = \lambda/7$, $\lambda_2 = 3\lambda/7$, $\lambda_3 = 3\lambda/7$; where λ_1, λ_2 and λ_3 are the call arrival rates for one-hop, two-hop and three-hop calls, respectively. And λ is the call arrival rate to a macrocell area. Hence the offered traffic are $\rho_1 = \lambda_1/\mu$, $\rho_2 = \lambda_2/\mu$ and $\rho_3 = \lambda_3/\mu$ for one-hop, two-hop and three-hop calls, respectively. $1/\mu$ is the average call duration. The offered traffic load per macrocell is given by $\rho = \lambda/\mu$ Erlangs.

For the seven-cell CMCN, the proposed FCA scheme can be modeled using a 13-dimensional Markov chain. The central microcell is assigned with N_0 channels and each of the six *virtual* microcells is assigned with N_1 channels. As shown in Figure 1(b), the seven microcells are numbered with 0, 1, 2, …, 6, starting from the central microcell. A state is defined as $(n_0^1, n_1^2, n_1^3, n_2^2, n_2^3, n_3^2, n_3^3, n_4^2, n_4^3, n_5^2, n_5^3, n_6^2, n_6^3)$. To make the analysis convenient, each state is numbered with an integer index s, and all the states form a set Π. For example, state s corresponds to a distinct sequence of nonnegative integers $(n_0^1(s), n_1^2(s), n_1^3(s), n_2^2(s), n_2^3(s), n_3^2(s), n_3^3(s), n_4^2(s), n_4^3(s), n_5^2(s), n_5^3(s), n_6^2(s), n_6^3(s))$ where $n_i^j(s)$ is number of j-hop calls in microcell i at state s. The permissible states must satisfy the following constraints:

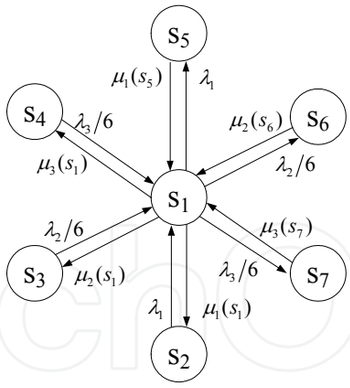

Fig. 7. Possible transitions for a state s_1.

$$\begin{cases} n_0^1(s)+2\times[n_1^2(s)+n_1^3(s)+n_2^2(s)+n_2^3(s)+n_3^2(s)+n_3^3(s) \\ +n_4^2(s)+n_4^3(s)+n_5^2(s)+n_5^3(s)+n_6^2(s)+n_6^3(s)]\le N_0 \\ 0\le n_0^1(s)\le N_0;\ \ 0\le 2n_i^2(s)\le N_0,\ 0\le n_i^3(s)\le N_1, \text{ for } i=1,2,\cdots,6 \end{cases} \tag{37}$$

A state transition can be caused by one of the following six events: an arrival/departure of a one-hop, two-hop or three-hop call. Applying the global-balance theory (Kleinrock, 1975), we can obtain one equation for each state. For example, for a state s_1 in Figure 7, we have,

$$\begin{aligned} &P(s_1)[\lambda_1+\lambda_2/6+\lambda_3/6+\mu_1(s_1)+\mu_2(s_1)+\mu_3(s_1)]=P(s_2)\lambda_1 \\ &+P(s_3)\lambda_2/6+P(s_4)\lambda_3/6+P(s_5)\mu_1(s_5)+P(s_6)\mu_2(s_6)+P(s_7)\mu_3(s_7) \end{aligned} \tag{38}$$

where $P(s)$ is the steady-state probability of state s, and $\mu_j(s)$ is the service rate for j-hop calls at state s. Similarly, the total state probability sums to unity,

$$\sum_{s\in\Pi}P(s)=1 \tag{39}$$

For a state set Π with m states, the array of global-balance equations form

$$[A]_{m\times m}[P]_{m\times 1}=[B]_{m\times 1} \tag{40}$$

$$[A]=\begin{bmatrix} 1 & 1 & \cdots & 1 \\ t_{21} & t_{22} & \cdots & t_{2m} \\ \vdots & \vdots & \cdots & \vdots \\ \vdots & \vdots & t_{ii} & \vdots \\ \vdots & \vdots & \cdots & \vdots \\ t_{m1} & t_{m2} & \cdots & t_{mm} \end{bmatrix},\ [P]=\begin{bmatrix} P(1) \\ P(2) \\ \vdots \\ P(i) \\ \vdots \\ P(m) \end{bmatrix},\ [B]=\begin{bmatrix} 1 \\ 0 \\ \vdots \\ 0 \end{bmatrix} \tag{41}$$

In matrix [A], there are two types of transition rates:
Transition Rates into a State: The element t_{ij} (when $i \neq j$) is the negative of the transition rate from state j to state i. The service rates for the three types of calls in microcell k from state j are $\mu_1(j)=n_0^1(j)\mu$, $\mu_2(j)=n_k^2(j)\mu$, $\mu_3(j)=n_k^3(j)\mu$, where k=1, 2, …, 6. Then we have,

$$t_{ij} = \begin{cases} -n_0^1(j)\mu, \text{ if } n_0^1(j) - n_0^1(i) = 1; & -\lambda_1, \text{if } n_0^1(j) - n_0^1(i) = -1; \\ -n_k^2(j)\mu, \text{if } n_k^2(j) - n_k^2(i) = 1; & -\lambda_2/6, \text{if } n_k^2(j) - n_k^2(i) = -1; \\ -n_k^3(j)\mu, \text{if } n_k^3(j) - n_k^3(i) = 1; & -\lambda_3/6, \text{if } n_k^3(j) - n_k^3(i) = -1; \\ 0, \text{ otherwise.} \end{cases} \quad (42)$$

Transition Rates out of a State: The element t_{ii} is equal to the sum of the transition rates out of state i. For state i, we have,

$$t_{ii} = -\sum_{j=1, j\neq i}^{m} t_{ji} \quad (43)$$

By solving the matrix equation, we can get the matrix [P]. Then, the blocking probabilities, P_{b1}, P_{b2} and P_{b3} for one-hop call, two-hop call and three-hop call in each cell are given by,

$$P_{b1} = \sum_{s\in\Pi} P(s)\Big|_{n_0^1(s)+2\times\sum_{i=1}^{6}[n_i^2(s)+n_i^3(s)]=N_0} \quad (44)$$

$$P_{b2} = \sum_{s\in\Pi} P(s)\Big|_{n_0^1(s)+2\times\sum_{i=1}^{6}[n_i^2(s)+n_i^3(s)]\geq N_0-1} \quad (45)$$

$$P_{b3} = P_{b2} + \frac{1}{6}\sum_{i=1}^{6}\sum_{s\in\Pi} P(s)\Big|_{n_i^3(s)=N_1} - \frac{1}{6}\sum_{i=1}^{6}\sum_{s\in\Pi} P(s)\Big|_{n_i^3(s)=N_1 \text{ and } n_0^1(s)+2\sum_{k=1}^{6}\left[n_k^2(s)+n_k^3(s)\right]\geq N_0-1} \quad (46)$$

The average call blocking probability, $P_{b,D}$, for downlink is given in (36).

The exact model may result in excessive long computational time, especially for large N_0 and N_1. To reduce the computational load, we find an approximated model with much fewer states to analyze the AFCA scheme and the detailed analysis is available in (Li & Chong, 2008).

3.2 Numerical results and discussions

First of all, we look at the validity of our analytical models for the proposed AFCA scheme. For the hypothetical two-cell CMCN, we do not assume any value of N. We have simply used any (N_0, N_1) channel combinations for a two-cell CMCN just for the purpose of validating the analytical model. These channel combinations (N_0, N_1) have no physical meaning for a two-cell CMCN. As shown in Figure 8, the simulation results match with the results obtained from the analytical model.

Then, we study the performance of the seven-cell CMCN. In this simulation study, we set the total number of system channels to be N = 70. For the seven-cell CMCN, we first look at the performance of uniform FCA, where each (central or *virtual*) microcell has equal number of channels with ($N_{U,c}$=10, $N_{U,v}$=10). The simulated system consists of one macrocell which is divided into seven microcells as shown in Figure 1(b). Calls arrive according to a Poisson process with a call arrival rate λ per macrocell. Call durations are exponentially distributed with a mean of $1/\mu$. Each simulation runs until 10 million calls are processed. The 95% confidence intervals are within ±10% of the average values shown.

Figure 9 shows the $P_{b,U}$ for seven CMCN with different (N_0, N_1) combinations. The performance of CMCN with (10, 10) has the same $P_{b,U}$ compared to SCNs, where a cell has

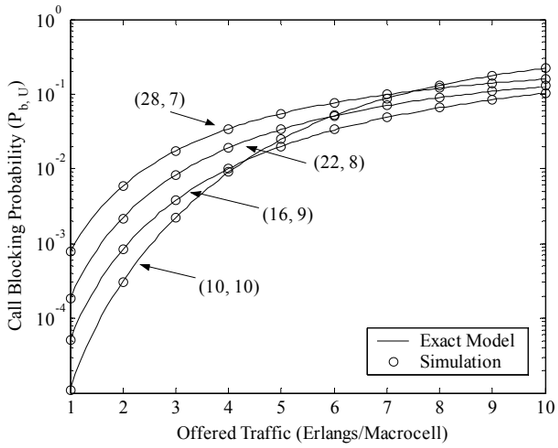

Fig. 8. Uplink performance of the hypothetical two-cell CMCN model.

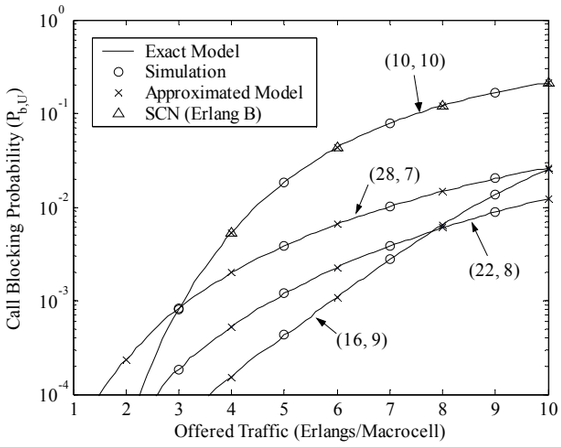

Fig. 9. Uplink performance of the AFCA for the seven-cell CMCN.

the same coverage area as the macrocell in CMCN, with 10 channels. This is expected because in CMCNs, every multihop call in the six surrounding *virtual* microcells will require one channel from the central microcell to access to the BS. In other words, the central microcell needs to support all the traffic from all seven microcells, which is equivalent to the traffic in a macrocell. Since N_1 is large enough in the *virtual* microcells, calls are rarely blocked due to insufficient channels in the *virtual* microcells. Thus, the bottleneck of the performance results with N_0 in the central microcell, which is used to support all the traffic in the seven microcells.

Next, we study the performance of CMCNs by increasing N_0 in the central microcell and reducing the N_1 in the six *virtual* microcells. Figure 9 shows the results of different channel combinations: (16, 9), (22, 8), (28, 7). From the results, it can be seen that our proposed CMCN with the AFCA scheme is able to reduce the $P_{b,U}$ significantly as compared to the SCNs. If $P_{b,U}$ is set at 1%, the AFCA scheme can support about 2 times more traffic. For example, the CMCN with (22, 8) supports 9.6 Erlangs; while a cell in SCNs only supports 4.5 Erlangs. Furthermore, the results obtained from the approximated model can provide a good estimation for the exact model. This again validates the correctness of both analytical models. Also, the simulation results match closely with the analytical results.

Table 1 shows the performance of the proposed CMCN with AFCA in different microcells under two channel combinations (10, 10) and (16, 9) at ρ=5 Erlangs. The number of call arrivals in different microcells is nearly the same because of uniform call arrivals. Performance in the six *virtual* microcells is statistically the same as they are homogenous. With (10, 10), the call blocking probability in microcell i, $P_{B,i,}$ is the same for all (central or *virtual*) microcells because the call blocked is due to insufficient channel in the central microcell. The call blocking probability, $P_{B,0}$ in central microcell 0 is about 0.0182 under (10, 10), while it is reduced to 5.39×10^{-5} under (16, 9). This is because the increase in N_0 can reduce the call probability in the central microcell greatly. For each of the six *virtual* microcells, with N_0 increasing from 10 to 16 and N_1 reducing from 10 to 9, $P_{B,i}$, i=1, 2, …, 6, also reduces sharply from 0.0182 to 5×10^{-4}. Since a multihop call not only occupies the channels in a *virtual* microcell, but also requires one channel from the central microcell, a multihop call can be blocked either by lack of channels in the central microcell or in a *virtual* microcell. More N_0 can provide connections to the calls originated from the *virtual* microcells so that $P_{B,i}$ of the *virtual* microcells is reduced.

scenario	Cell No.	No. of call arrival	No. of blocked calls	$P_{B,i}$	blocked calls due to insufficient channels in its own microcell	$P_{B\text{-}own,i}$
(10, 10)	0	1427909	25930	0.018159	25930	1.0
	1	1427448	25818	0.018087	77	0.002982
	2	1430117	26406	0.018464	61	0.00231
	3	1428187	26161	0.018318	44	0.001682
	4	1427711	25985	0.0182	60	0.002309
	5	1428577	26211	0.018348	51	0.001946
	6	1430051	26130	0.018272	58	0.00222
(16, 9)	0	1428030	77	5.39e-5	77	1.0
	1	1427287	721	5.05e-4	663	0.919556
	2	1430237	736	5.15e-4	658	0.894022
	3	1428246	647	4.53e-4	580	0.896445
	4	1427483	668	4.68e-4	614	0.919162
	5	1428799	693	4.85e-4	633	0.91342
	6	1429918	733	5.13e-4	664	0.905866

Table 1. Call blocking with different (N_0, N_1) combinations at ρ=5 Erlangs.

Furthermore, we define another parameter, $P_{B\text{-}own,i}$, which denotes the percentage that a blocked call is due to the lack of channels in microcell i. For $P_{B\text{-}own,0}$, all the calls blocked in the central microcell are due to lack of free channels in the central microcell. Thus, $P_{B\text{-}own,0}$ is 1. Table 1 shows that under (10, 10), multihop calls are rarely blocked due to lack of channels in their own *virtual* microcells because of sufficient channels in the *virtual* microcells; while under (16, 9) most of the multihop blocked call is due to lack of channels in their own *virtual* microcells.

The call blocking probabilities, P_{b1}, P_{b2} and P_{b3}, with different channel combinations for different ρ are shown in Figure 10. We notice that the P_{b1}, P_{b2} and P_{b3} are about the same under (10, 10), which is due to the fact that all types of calls are blocked for the same

reason—inadequate channels are allocated to the central microcell. As we increase N_0 by 6 and slightly reduce N_1 by 1, the P_{b2} and P_{b3} are reduced because more channels in central microcell provide more channels for setting up connections for the two-hop and three-hop calls. P_{b3} is higher than P_{b2} because three-hop calls require one more channel than two-hop calls from its *virtual* microcell. For channel combination of (28, 7), as there are adequate channels available in the central microcell, P_{b1} is close to zero. P_{b2} and P_{b3} for (28, 7) are higher than those for (16, 9) because there are not enough channels in the *virtual* microcells to support multihop calls. Thus, N_1 will limit the QoS of the multihop calls. Beyond the optimum combination, if we further reduce N_1 and increase N_0, the performance will be degraded because more calls will be blocked in the *virtual* microcells.

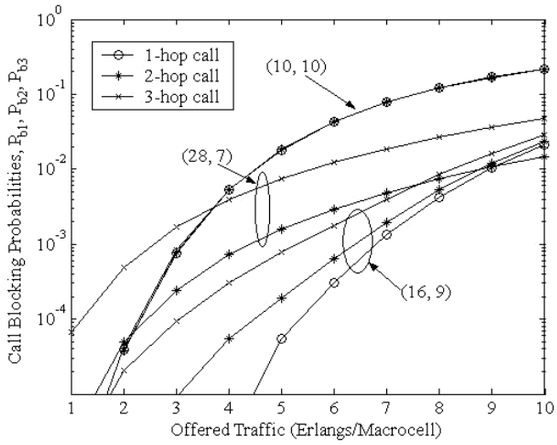

Fig. 10. Uplink call blocking probability for different types of calls.

For the hypothetical two-cell CMCN, analytical results match closely with the simulation results, which are not shown here because they are of less importance as compared to that of the seven-cell CMCN.

Figure 11 shows the downlink call blocking probability, $P_{b,D}$, for the seven-cell CMCN with different (N_0, N_1) for downlink transmission. We study the performance of CMCN by increasing N_0 in the central microcell and reducing the N_1 in the six *virtual* microcells. For the CMCNs, more channels are required from the central microcell for downlink transmission. Therefore, we can reduce the $P_{b,D}$ by increasing N_0. With N=70 and N_r=7 for uniform FCA in SCNs, each macrocell has 10 channels. From the Erlang B formula, the amount of traffic it can support at $P_{b,D}$ = 1% is about 4.5 Erlangs. For our CMCN, after dividing the macrocell into one central microcell and six *virtual* microcells, with channel combination of (34, 6), it can support about 10.5 Erlangs and the improvement factor is larger than 130%. We find that the optimum combination is (46, 4) and the capacity at $P_{b,D}$ = 1% is 14.2 Erlangs. If N_0 continues to increase by reducing N_1 after (46, 4), the capacity begins to decrease such as (52, 3) because there is not enough channels in surrounding *virtual* microcells to handle the traffic. Furthermore, the results obtained from the approximated model can provide a good estimation for the exact model. This again validates the correctness of both analytical models. Also, the simulation results match closely with the analytical results.

The capacity for CMCN, shown in Figure 11 is entirely based on the $P_{b,D}$. Since uplink and downlink channel assignment is different in CMCN, the system capacity will be different

depending on (N_0, N_1) for uplink or downlink. We define the system call blocking probability, $P_{b,s}$, as the probability of lacking of either uplink or downlink channels for a new call. As uplink channel assignment and downlink channel assignment are independent, $P_{b,s}$ is mathematically equal to the larger value between $P_{b,U}$ and $P_{b,D}$. Figure 11 shows $P_{b,s}$ for uplink channel combination, UL($N_{U,c}$=10, $N_{U,v}$=10), with different downlink channel combination, DL($N_{D,c}$=N_0, $N_{D,v}$=N_1). For UL(10, 10) and DL(10, 10), it has the highest $P_{b,s}$. As we increase N_0 in the downlink channel combination, the system capacity at $P_{b,s}$ = 1% is increased. This is because $P_{b,D}$ is higher than uplink blocking probability, $P_{b,U}$, and thus, the system capacity is limited by downlink channel combination. However, further increase in N_0 for the central microcell in the downlink channel combination, such as increasing N_0 from 22 to 28, no more capacity is increased. This is because $P_{b,U}$ of UL(10, 10) is higher than $P_{b,D}$ for DL(28, 7), and the capacity is limited by UL(10, 10). Thus, further increase in N_0 in the downlink channel combination will not improve the capacity.

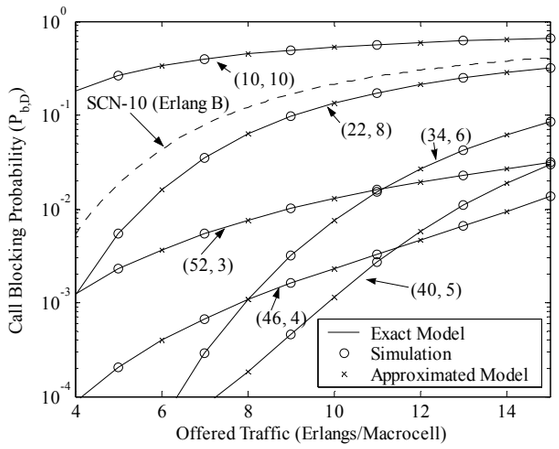

Fig. 11. Downlink performance of the AFCA for the seven-cell CMCN.

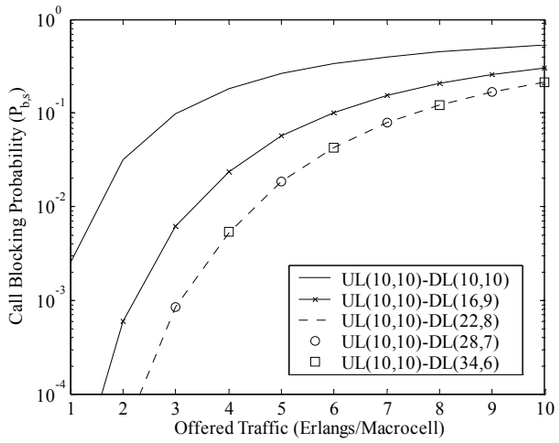

Fig. 12. Call blocking probability with both uplink and downlink transmissions.

Finally, we study the system capacity supported by the proposed AFCA scheme for uplink and downlink transmissions at $P_{b,s}$ = 1%. Table 2 shows the different values of system capacity supported by possible (N_0, N_1) for uplink or downlink. For symmetric FCA, if we

use (10, 10) for both uplink and downlink channel combinations, the system capacity is 1.53 Erlangs, which is limited by the downlink capacity, as shown in Figure 11. Nevertheless, if we use (46, 4) instead of (10, 10) for both uplink and downlink channel combinations, the system capacity is 1.36 Erlangs, which is limited by the uplink capacity. From Table 2, it can be seen that the maximum capacity supported by symmetric FCA is about 6.92 Erlangs with (28, 7) for both uplink and downlink channel combinations. Therefore, we need to make use of the AFCA, in which the channel combinations (N_0, N_1) for uplink and downlink are different, in order to achieve larger system capacity. From Table 2, we suggest that with channel combination of UL(22, 8) and DL(34, 6) for downlink, the maximum system capacity can be obtained to be as large as 9.31 Erlangs. Beyond the optimum combination, if we further reduce N_1 and increase N_0, the performance will be degraded because more calls will be blocked in the *virtual* microcells.

Combinations (N_0, N_1)	Uplink Capacity (Erlangs)	Downlink Capacity (Erlangs)
(10, 10)	4.43	1.53
(16, 9)	8.51	3.33
(22, 8)	9.31	5.55
(28, 7)	6.92	7.89
(34, 6)	4.88	10.46
(40, 5)	2.92	12.92
(46, 4)	1.36	14.21
(52, 3)	0.33	9.08

Table 2. System capacity for uplink and downlink vs. channel combinations.

4. Proposed dynamic channel assignment scheme

Abovementioned results show that CMCN with AFCA can improve the system capacity. However, FCA is not able to cope with temporal changes in the traffic patterns and thus may result in deficiency. Moreover, it is not easy to obtain the optimum channel combination under the proposed AFCA, which is used to achieve the maximum system capacity. Therefore, dynamic channel assignment (DCA) is more desirable.

We proposed a multihop dynamic channel assignment (MDCA) scheme that works by assigning channels based on the interference information in the surrounding cells (Chong & Leung, 2001).

4.1 Multihop dynamic channel assignment

Figure 13 also shows the three most typical channel assignment scenarios:

1) One-hop Calls: One-hop calls refer to those calls originated from MSs in a central microcell, such as MS_1 in microcell A in Figure 13. It requires one uplink channel and one downlink channel from the microcell A. The call is accepted if microcell A has at least one free uplink channel and one free downlink channel. Otherwise, the call is blocked.

2) Two-hop Calls: Two-hop calls refer to those calls originated from MSs in the inner half region of a *virtual* microcell, such as MS_2 in region B_1 of microcell B in Figure 13. The BS is able to find another MS, RS_0, in the central microcell acting as a RS. For uplink transmission, a two-hop call requires one uplink channel from the microcell B, for the transmission from MS_2 to RS_0, and one uplink channel from the central microcell A, for the transmission from

RS_0 to the BS. For downlink transmission, a two-hop call requires two downlink channels from the central microcell *A*, for the transmission from the BS to RS_0, and from RS_0 to MS_2, respectively. A two-hop call is accepted if all the following conditions are met: (i) there is at least one free uplink channel in microcell *B*; (ii) there is at least one free uplink channel in the central microcell *A*; and (iii) there are at least two free downlink channels in the central microcell *A*. Otherwise, the call is blocked.

3) Three-hop Calls: Three-hop calls refer to those calls originated from MSs in the outer half region of a *virtual* microcell, such as MS_3 in region B_2 of microcell *B* in Figure 13. The BS is responsible for finding two other MSs, RS_1 and RS_2, to be the RSs for the call; RS_1 is in the central microcell *A* and RS_2 is in the region B_1. For uplink transmission, a three-hop call requires two uplink channels from microcell *B* and one uplink channel from the central microcell *A*. The three uplink channels are used for the transmission from MS_3 to RS_2, from RS_2 to RS_1 and RS_1 to the BS, respectively. For downlink transmission, a three-hop call requires two downlink channels from central microcell *A* and one downlink channel from microcell *B*. A three-hop call is accepted if all the following conditions are met: (i) there is at least one free uplink channel in the central microcell *A*; (ii) there at least two free uplink channels in the microcell *B*; (iii) there are at least two free downlink channels in the central microcell *A*; and (iv) there is at least one free downlink channel in microcell *B*. Otherwise, it is blocked.

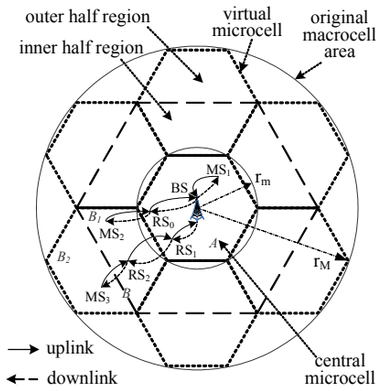

Fig. 13. Channel assignment in CMCN.

The channel assignment in CMCN to a call for the uplink and downlink is unbalanced. This is different from that in SCNs, where same number of channels is allocated to a call for uplink and downlink. Under the asymmetric FCA (AFCA) for CMCN (Li & Chong, 2006), each *virtual* or central microcell is allocated a fixed number of channels. The uplink and downlink channel combination are UL($N_{U,c}$, $N_{U,v}$) and DL($N_{D,c}$, $N_{D,v}$), respectively, where $N_{U,c}/N_{D,c}$ and $N_{U,v}/N_{D,v}$ are the number of uplink/downlink channels in the central and *virtual* microcells, respectively. The channel assignment procedure of AFCA is presented in Section 1.3, hence not revisited here.

4.2 Interference information table

The proposed MDCA scheme works on the information provided by the Interference Information Table (IIT) (Chong & Leung, 2001). Two global IITs are stored in mobile switching center (MSC) for the uplink and downlink channels. The channel assignment is conducted and controlled by the MSC, instead of a BS, because a MSC has more

computational resource than a BS. This features a centralized fashion of MDCA, which results more efficient usage of the system channel pool. Consequently, the BS will only assign/release channels based on the instruction from the MSC.

Denote the set of interfering cells of any microcell A as $I(A)$. The information of $I(A)$ is stored in the Interference Constraint Table (ICT). ICT is built based on the cell configuration with a given reuse factor, N_r. For a given microcell A, different reuse factor N_r values will lead to different $I(A)$. Thus, we can implement MDCA with any N_r by changing $I(A)$ information in the ICT. For example, with N_r = 7 the number of interfering cells in $I(A)$ is 18, which includes those interfering cells in the first and second tiers. For example, Table 4 shows the ICT for the simulated network in Figure 14 with N_r = 7. Refer to Table 4, the cell number corresponds to the cell coverage of each cell in Figure 14.

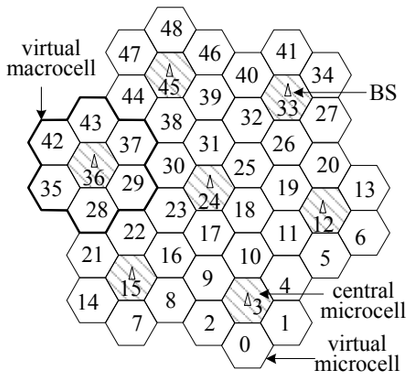

Fig. 14. The simulated 49-cell network.

	Channel				
Cell	1	2	3	…	N
0	L	L	2L	…	L
1		2L	U_{22}	…	U_{33}
2	L	L	2L	…	2L
3	L	U_{11}	2L	…	L
…	…	…	…	…	…
12		U_{11}	U_{11}	…	L
…	…	…	…	…	…
48	U_{22}	L	U_{33}	…	

Table 3. Interference Information Table for uplink.

Table 3 shows the uplink IIT for the CMCN shown in Figure 14, which includes the shared N system uplink channels in each cell. The downlink IIT is similar and hence not illustrated here. The content of an IIT is described as follows.

1) Used Channels: a letter '$U_{11/22/33}$' in the (microcell A, channel j) box signifies that channel j is a used channel in microcell A. The subscript indicates which hop the channel is used for; 'U_{11}', 'U_{22}', 'U_{33}' refer to the first-hop channel, the second-hop channel and the third-hop channel, respectively. The first-hop channel refers to the channel used between the BS and the destined MS inside the central microcell. The second-hop channel refers to the channel used between the MS (as a RS) in the central microcell and the destined MS in the inner half

of the *virtual* microcell. The third-hop channel refers to the channel used between the MS (as a RS) in the inner half of the *virtual* microcell and the destined MS in the outer half of the *virtual* microcell.

2) Locked Channels: a letter 'L' in (microcell *A*, channel *j*) box signifies that microcell *A* is not allowed to use channel *j* due to one cell in *I*(*A*) is using channel *j*. Similarly, '*n*L' in (microcell *A*, channel *j*) box indicates *n* cells in *I*(*A*) are using channel *j*.

3) Free Channels: an empty (microcell *A*, channel *j*) box signifies that channel *j* is a free channel for microcell *A*.

Cell	Central Microcell	Interfering Cells				
		1	2	3	…	18
0	3	40	46	2	…	34
1	3	41	0	3	…	28
2	3	46	48	8	…	41
…	…	…	…	…	…	…
48	45	45	47	7	…	40

Table 4. Interference Constraint Table for the simulated network.

4.3 Channel searching strategies

1) Sequential Channel Searching *(SCS)*: When a new call arrives, the SCS strategy is to always search for a channel from the lower to higher-numbered channel for the first-hop uplink transmission in the central microcell. Once a free channel is found, it is assigned to the first-hop link. Otherwise, the call is blocked. The SCS strategy works in the same way to find the uplink channels for second- or third-hop links for this call if it is a multihop call. The channel searching procedure is similar for downlink channel assignment as well.

2) Packing-based Channel Searching (PCS): The PCS strategy is to assign microcell *A* a free channel *j* which is locked in the largest number of cells in *I*(*A*). The motivation behind PCS is to attempt to minimize the effect on the channel availability in those interfering cells. We use *F*(*A, j*) to denote the number of cells in *I*(*A*) which are locked for channel *j* by cells not in *I*(*A*). Interestingly, *F*(*A, j*) is equal to the number of cells in *I*(*A*) with a label '*L*' in channel *j*'s column in the IIT. Then the cost for assigning a free channel *j* in microcell *A* is defined as

$$E(A, j) = I(A) - F(A, j) \tag{47}$$

This cost represents the number of cells in *I*(*A*) which will not be able to use channel *j* as a direct result of channel *j* being assigned in microcell *A*. Mathematically, the PCS is to

$$\min_j E(A, j) = I(A) - F(A, j) \text{ subject to: } \quad 1 \le j \le N. \tag{48}$$

Since *I*(*A*) is a fixed value for a given N_r, the problem can be reformulated as

$$\max_j F(A, j) = \sum_{X \in I(A)} \delta(X, j) \text{ subject to: } \quad 1 \le j \le N. \tag{49}$$

where $\delta(X, j)$ is an indicator function, which has a value of 1 if channel *j* is locked for microcell *X* and 0 otherwise. Specifically, to find a channel in microcell *A,* the MSC checks

through the N channels and looks for a free channel in microcell A that has the largest $F(A, j)$ value. If there is more than one such channel, the lower-numbered channel is selected. For example, Table 5 shows a call in cell 15 requesting a first-hop channel. Channels 1, 2 and 3 are the three free channels in cell 15. Refer to , $I(15)$ = [2, 7, 8, 9, 13, 14, 16, 17, 20, 21, 22, 23, 27, 28, 29, 34, 47, 48] with N_r = 7. Since most of the cells in $I(15)$ are locked for channel 2, it is suitable to assign channel 2 as the first-hop channel in cell 15 because $F(15, 2) = 15$ is largest among the $F(15, j)$ values for j = 1, 2 and 3.

The best case solution is when $E(A, j) = 0$. However, it might not be always feasible to find such a solution. The proposed PCS strategy attempts to minimize the cost of assigning a channel to a cell that makes $E(A, j)$ as small as possible. Thus, it results in a sub-optimal solution.

	Channel				
Cell	1	2	3	...	N
…	…	…	…	…	…
2		L		…	L
…	…	…	…	…	…
7		L		…	L
8		L		…	L
9	L	L		…	2L
…	…	…	…	…	…
13		L		…	L
14		2L		…	L
15				…	U_{11}
16	L	L		…	2L
17	L	L		…	2L
….	…	…	…	…	…
20		2L		…	L
21		L		…	L
22	L			…	2L
23	L			…	2L
…	…	…	…	…	…
27		2L		…	L
28		L		…	L
29	L			…	2L
…	…	…	…	…	…
34		L		…	L
…	…	…	…	…	…
47		L		…	L
48		L	2L	…	L

Table 5. Packing-based Channel Searching for uplink.

Consider an uplink IIT and a downlink IIT with C cells and N uplink and N downlink channels. The cell of interest is cell m. The worst case scenario for channel assignment using the SCS strategy is for a three-hop call when there are only three free channels with the largest channel numbers left in cell m. The channel searching for the first-hop link requires N-2 operations. Similarly, the second-hop and third-hop links require N-1 and N operations, respectively. Next, for channel updating, the MSC needs to update 19 microcells (its own cell and 18 surrounding cells) with a total of 19 channel entries for each assigned channel. Then, a total of 19×3=57 steps are required for a three-hop call set-up. Finally, after the call is completed, another 57 steps are required for channel updates. Therefore, in the worst case scenario, a three-hop call requires a total of 3(N-1)+57×2, i.e. 3(N+37) steps. Therefore, the worst case algorithm complexity (Herber, 1986) for the SCS strategy is approximated to be O(3N). The number of operations required for the uplink and downlink are the same.

The worst case algorithm complexity for the PCS strategy with N_r is estimated to be O(12(N-1)[f(N_r)+1]) (Herber, 1986), where f(N_r) is number of cells in I(A) for cell A with a given N_r (e.g. when N_r = 7, f(N_r) = 18). This worst case algorithm complexity is calculated by estimating the number of steps required to assign channels to a three-hop call when all N channels are free. A three-hop call requires three uplink channels and three downlink channels. First, for a first-hop uplink, it takes N steps to check the channel status of all N channels in microcell A. Then, it takes 2f(N_r) steps to check the entry for each cell in I(A) for a *free* channel j to calculate F(A, j). Since all N channels are free, the total number of steps to obtain F(A, *) for all N channels is 2f(N_r)N. Finally, it takes N-1 steps to compare the N F(A, *) values and find the largest F(A, *). Similarly, the same approach can be applied for second- and third-hop uplink to obtain F(B, *) and the complexity for uplink channel assignment is given by

$$O\left(\begin{Bmatrix}[N+2f(N_r)N+N-1]\\ +[N-1+2f(N_r)(N-1)+N-2]\\ +[N-2+2f(N_r)(N-2)+N-3]\end{Bmatrix}\right)=O\left(6(N-1)\left[f(N_r)+1\right]\right) \tag{50}$$

Since the computational complexity for downlink is the same as uplink, the total worst case algorithm complexity is simply equal to O(12(N-1)[f(N_r)+1]).

4.4 Channel updating

1) Channel Assignment: when the MSC assigns the channel j in the microcell A to a call, it will (i) insert a letter '$U_{11/22/33}$' with the corresponding subscript in the (microcell A, channel j) entry box of the IIT; and (ii) update the entry boxes for (I(A), channel j) by increasing the number of 'L'.

2) Channel Release: when the MSC releases the channel j in the microcell A, it will (i) empty the entry box for (microcell A, channel j); and (ii) update the entry boxes for (I(A), channel j) by reducing the number of 'L'.

4.5 Channel reassignment

When a call using channel i as a k^{th}-hop channel in microcell A is completed, that channel i is released. The MSC will search for a channel j, which is currently used as the k^{th}-hop channel

of an ongoing call in microcell A. If $E(A, i)$ is less than $E(A, j)$, the MSC will reassign channel i to that ongoing call in microcell A and release channel j. CR is only executed for channels of the same type (uplink/downlink) in the same microcell. Thus, CR is expected to improve the channel availability to new calls. Mathematically, the motivation behind CR can be expressed as a reduction in the cost value:

$$\Delta E(A, i \to j) = E(A, i) - E(A, j) = F(A, j) - F(A, i) < 0 \tag{51}$$

4.6 Simulation results

The simulated network of an area consisting of 49 microcells is shown in Figure 15. The wrap-around technique is used to avoid the boundary effect (Lin & Mak, 1994), which results from cutting off the simulation at the edge of the simulated region. In reality, there are interactions between the cells outside the simulated region and the cells inside the simulated region. Ignorance of these interactions will cause inaccuracies in the simulation results. For example, in Figure 15, the shaped microcell 30 has 6 neighbor cells, while a boundary cell, e.g., the shaped microcell 42 has only 3 neighbor cells. Wrap-around technique "wraps" the simulation region such that the left side is "connected" to the right side and similarly for other symmetric sides. For example, for a hexagonal-shaped simulation region, there will be three pair of sides and they will be "connected" after applying the wrap-around technique. With wrap-around technique, in Figure 15, microcells 1, 4 and 5 will become "neighbor cells" (I & Chao, 1993) to microcell 42. Similar technique applies to other boundary cells. In this way, each of the microcells will have 6 "neighbor cells". Thus, the boundary effect is avoided.

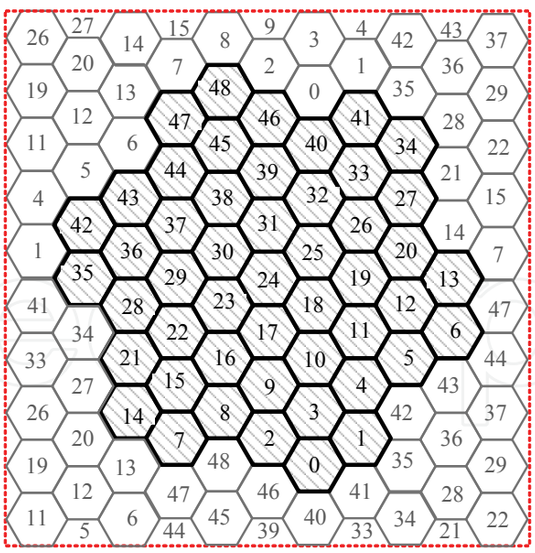

Fig. 15. The simulated network with wrap-around.

The number of system channels is N=70 (70 uplink channels and 70 downlink channels). We use N_r=7 as illustration, hence a channel used in cell A cannot be reused in the first and the second tier of interfering cells of A, i.e. two-cell buffering. Two traffic models are studied: the uniform traffic model generates calls which are uniformly distributed according to a

Poisson process with a call arrival rate λ per macrocell area, while the hot-spot traffic model only generates higher call arrival rate in particular microcells. Call durations are exponentially distributed with a mean of $1/\mu$. The offered traffic to a macrocell is given by $\rho=\lambda/\mu$. Each simulation runs until 100 million calls are processed. The 95% confidence intervals are within ±10% of the average values shown. For the FCA in SCNs, the results are obtained from Erlang B formula with $N/7$ channels per macrocell.

4.6.1 Simulation results with uniform traffic

Figure 16 shows both the uplink and downlink call blocking probability, i.e. $P_{b,U}$ and $P_{b,D}$. Notice that the $P_{b,U}$ is always higher than the $P_{b,D}$ due to the asymmetric nature of multihop transmission in CMCN that downlink transmission takes more channels from the central microcell than uplink transmission. The channels used in the central microcells can be reused in the other central microcells with minimum reuse distance without having to be concerned about the co-channel interference constraint, because two-cell buffering is already in place. The system capacity based on $P_{b,U}$ = 1% for MDCA with SCS and PCS are 15.3 and 16.3 Erlangs, respectively. With PCS-CR (channel reassignment), the capacity of MDCA is increased by 0.4 Erlangs.

Figure 17 shows the average call blocking probabilities for FCA and DCA-WI for SCNs (Chong & Leung, 2001), AFCA for CMCN (Li & Chong, 2006), MDCA with SCS, PCS and PCS-CR. DCA-WI, known as DCA with interference information, is a distributed network-based DCA scheme for SCNs. Under DCA-WI, each BS maintains an interference information table and assigns channels according to the information provided by the table. Only the $P_{b,U}$ for MDCA is shown because uplink transmission has lower capacity. At $P_{b,U}$ = 1%, the system capacity for the FCA and DCA-WI are 4.5 Erlangs and 7.56 Erlangs, respectively. AFCA with optimum channel combinations, UL($N_{U,c}$=22, $N_{U,v}$=8) and DL($N_{D,c}$=40, $N_{D,v}$=5), can support 9.3 Erlangs. The MDCA with SCS, PCS, and PCS-CR can support 15.3 Erlangs, 16.3 Erlangs and 16.7 Erlangs, respectively. As compared to DCA-WI and AFCA, the improvements of MDCA with PCS-CR are 120.9% and 79.6%, respectively.

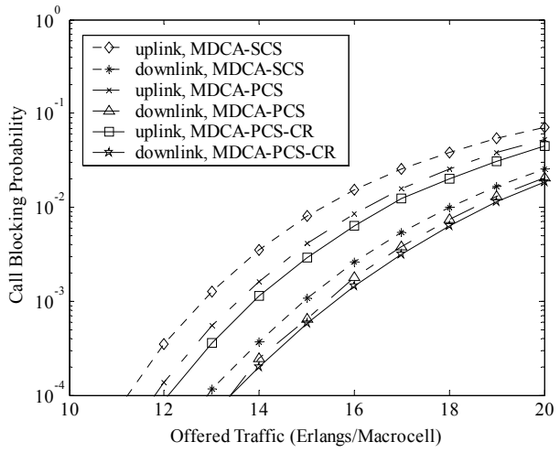

Fig. 16. Asymmetric capacity for uplink and downlink for CMCN using MDCA.

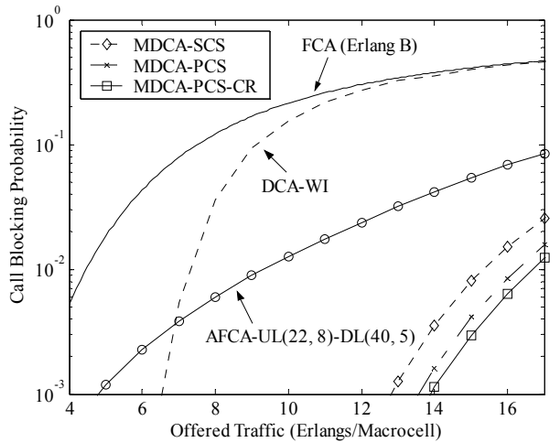

Fig. 17. Capacity comparison with N=70.

Figure 18 shows the uplink blocking probabilities, P_{b1}, P_{b2} and P_{b3}, for one-hop, two-hop and three-hop calls respectively. As expected, P_{b3} is generally higher than P_{b2}, and P_{b2} is higher than P_{b1}. The blocking probabilities for the three types of calls are lower for MDCA when using the PCS strategy as opposed to the SCS strategy. This is because the PCS strategy improves the channel availability and thus reduces the blocking probabilities of the three types of calls. The PCS-CR is not included in Figure 18 because the purpose CR will simply enhance the advantage of PCS by minimizing the effect of assigning a channel on the channel availability of the whole system.

Figure 19 illustrates the performance of MDCA with a larger number of system channels, when N=210. The Erlang B formula calculates that a SCN with N=210 can support only 20.3 Erlangs. The capacity for DCA-WI is 25.2 Erlangs. The capacity of CMCN with the optimum AFCA channel combination AFCA-UL(72, 23)-DL(144, 11) is 54.4 Erlangs at $P_{b,U}$ =1%. The MDCA using the SCS, PCS and PCS-CR strategies can support 61.5 Erlangs, 62.7 Erlangs and 63.7 Erlangs, respectively. Therefore, the MDCA sustains its advantage over conventional FCA, network-based DCA for SCNs and AFCA even for a large number of system channels.

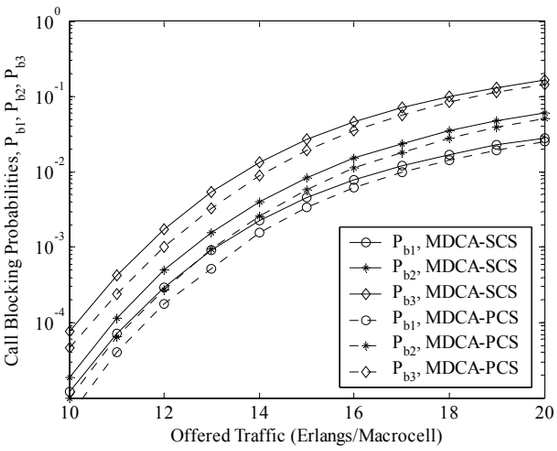

Fig. 18. Call blocking probability for different types of calls.

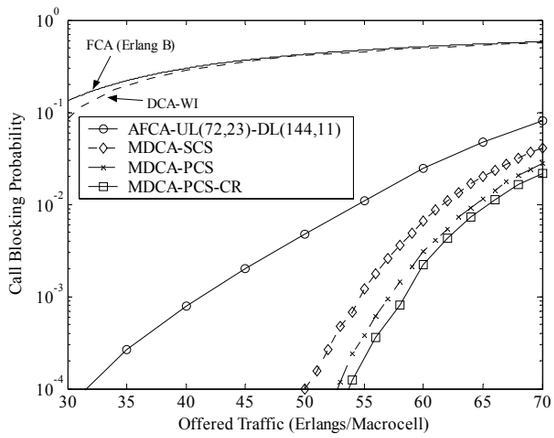

Fig. 19. Capacity comparison with N=210.

4.6.2 Simulation results with hot-spot traffic

First, as in (I & Chao, 1993), we adopted the same methodology to study the performance of MDCA with the static hot-spot traffic. Two scenarios are simulated. As shown in Figure 20, microcell 24 is chosen for the *isolated one hot-spot model* and microcells 2, 9, 17, 24, 31, 39, 46 are chosen to form the *expressway model*. First, each of the seven macrocells is initially loaded with a fixed nominal amount of traffic, which would cause 1% blocking if the conventional FCA were used. Next, we increase the traffic load in hot-spot microcells until the call blocking in any hot-spot microcell reaches 1%. Then we can obtain the capacity values for the hot-spot microcells areas.

With N = 70, each of the seven macrocells will be initially loaded at 4.46 Erlangs. In other words, each microcell is loaded with 0.637 Erlangs. We increase the traffic load for hot-spot cells, while keeping the traffic in non-hot-spot microcells at 0.637 Erlangs/Microcell. As shown in Figure 21, for the *isolated one hot-spot model*, FCA, AFCA and MDCA supports about 0.6 Erlangs, 9 Erlangs and 38 Erlangs per microcell, respectively. For the *expressway model*, FCA, AFCA and MDCA supports about 0.6 Erlangs, 1 Erlangs and 6 Erlangs per microcell, respectively. It can be seen that MDCA has a huge capacity to alleviate the blocking in hot-spot cells.

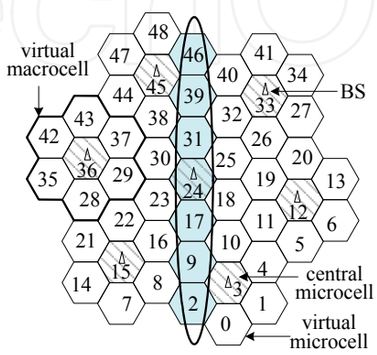

Fig. 20. The simulated hot-spot traffic cell model.

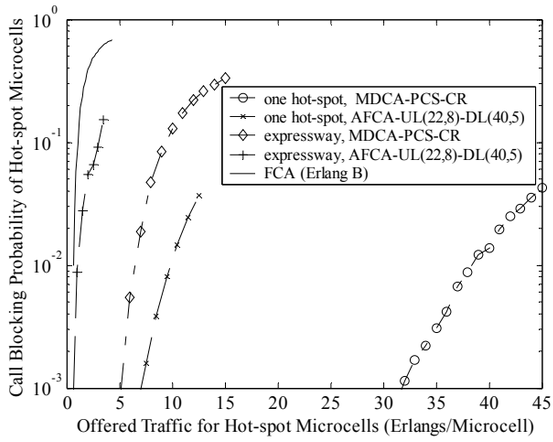

Fig. 21. Capacity comparison with hot-spot traffic for *N*=70.

Significant capacity improvements of MDCA have been observed with a larger *N*, e.g. *N* = 210, with uniform and hop-spot traffic. Same conclusion can be drawn that MDCA has a huge capacity to alleviate the blocking in hot-spot cells.

Finally, we investigate the performance of MDCA with a dynamic hot-spot traffic scenario and compare MDCA with AFCA. Under this traffic model, 7 hot-spot microcells are randomly selected from the 49 microcells shown in Figure 15. During the simulation, each data point is obtained by simulating the channel assignment for a period of with 1000 million calls. This period is divided into 10 equal intervals. For each interval, 7 hot-spot microcells are dynamically distributed over the 49-cell network by random selection. The average call blocking statistics are collected from the 7 hot-spot microcells from each interval. Notice that the selection of 7 hot-spot microcells is conducted for every interval and no two intervals will use the identical set of hot-spot microcells. At the end of the

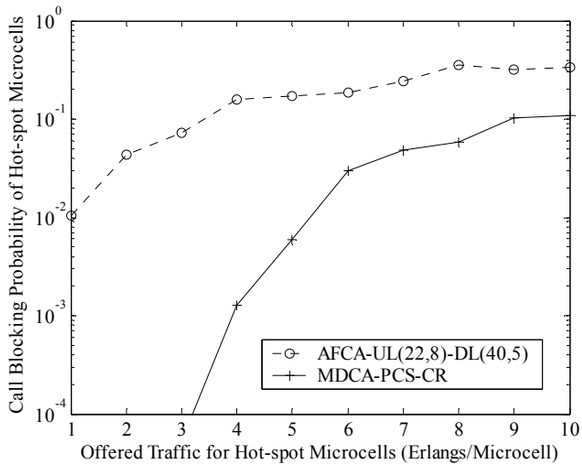

Fig. 22. Capacity comparison with dynamic hot-spot traffic for *N*=70.

simulation, we calculate the average call blocking probability over the 10 intervals. The traffic load in those non-hot-spot microcells is always 0.637 Erlangs/microcells according to the static hot-spot traffic model.

Figure 22 shows the capacity results for AFCA and MDCA with the dynamic hot-spot traffic scenario with N = 70 channels. MDCA and AFCA supports about 5.2 Erlangs and 1.0 Erlangs, respectively, at 1% call blocking. We can see that MDCA outperforms AFCA due to its flexibility of handling dynamic traffic distribution.

5. Conclusion

Clustered multihop cellular network (CMCN) is proposed as a compliment to *traditional* single-hop cellular networks (SCNs). A channel assignment, namely asymmetric fixed channel assignment (AFCA) is further proposed for the use in CMCNs. To analyze its performance, we have developed two multi-dimensional Markov chain models, including an exact model and an approximated model. The approximated model results in lower computational complexity and provides a good accuracy. Both models are validated through computer simulations and they matched with each other closely. Results show that the CMCN AFCA can increase the spectrum efficiency significantly. The system capacity can be improved greatly by increasing the number of channels assigned to the central microcell and decreasing the number of channels in the surrounding microcells. With optimum channel combination in the CMCN, the capacity can be doubled as compared to *traditional* SCNs.

We continued to investigate the feasibility of applying DCA scheme for MCN-type systems. A multihop DCA (MDCA) scheme with two channel searching strategies is proposed for clustered MCNs (CMCNs). Then, the computational complexity of the proposed MDCA with the two channel searching strategies is analyzed. A channel reassignment procedure is also investigated. Results show that MDCA can improve the system capacity greatly as compared to FCA and DCA-WI for SCNs and AFCA for CMCNs. Furthermore, MDCA can efficiently handle the hot-spot traffic.

In our analysis of fixed channel assignment scheme, we assumed that the MS population is infinite and RSs can be always found when a two-hop or three-hop call is concerned. Note that depending on the MS density, there would actually be an associated probability of finding a RS. It will cause serious difficulties with the analysis to incorporate the associated probability of finding a RS into the analytical models. Therefore, it has been left as part of our future work.

6. Reference

Adachi, Tomoko, & Nakagawa, Masao, (1998). A Study on Channel Usage in a Cellular-Ad-Hoc United Communication System for Operational Robots. *IEICE Transactions on Communications*. Vol. E81-B, No. 7 (July 1998), pp. 1500-07.

Aggelou, George Neonakis, & Tafazolli, Rahim, (2001). On the Relaying Capability of Next Generation Gsm Cellular Networks. *IEEE Personal Communications*. Vol. 8, No. 1 (February 2001), pp. 40-47.

Chong, P. H. J., & Leung, Cyril (2001). A Network-Based Dynamic Channel Assignment Scheme for Tdma Cellular Systems. *International Journal of Wireless Information Networks*. Vol. 8, No. 3 (July 2001), pp. 155-65.

Herber, S. Wilf. (1986). *Algorithms and Complexity*. 1st ed. Prentice-Hall, New Jersey, USA.

Hsu, Yu-Ching, & Lin, Ying-Dar, (2002). Multihop Cellular: A Novel Architecture for Wireless Data Communications. *Journal of Communications and Networks*. Vol. 4, No. 1 (March 2002), pp. 30-39.

I, Chih-Lin, & Chao, Pi-Hui. (1993). Local Packing - Distributed Dynamic Channel Allocation at Cellular Base Station. In Proceedings of IEEE GLOBECOM'93 (Houston, TX, USA, 29 November - 2 December 1993). 1, 293-301.

Kleinrock, Leonard. (1975). *Queueing System* 1st ed. John Wiley & Sons, New York.

Kudoh, E., & Adachi, F., (2005). Power and Frequency Efficient Wireless Multi-Hop Virtual Cellular Concept. *IEICE Transactions on Communications*. Vol. E88B, No. 4 (Apr 2005), pp. 1613-21.

Li, Xue Jun, & Chong, P. H. J., (2008). Asymmetric Fca for Downlink and Uplink Transmission in Clustered Multihop Cellular Network. *Wireless Personal Communications*. Vol. 44, No. 4 (March 2008), pp. 341-60.

---. (2006). A Fixed Channel Assignment Scheme for Multihop Cellular Network. In Proceedings of IEEE GLOBECOM'06 (San Francisco, CA, USA, 27 November - 1 December 2006). WLC 20-6, 1-5.

---, (2010). Performance Analysis of Multihop Cellular Network with Fixed Channel Assignment. *Wireless Networks*. Vol. 16, No. 2 (February 2010), pp. 511-26.

Lin, Yi-Bing, & Mak, Victor W., (1994). Eliminating the Boundary Effect of a Large-Scale Personal Communication Service Network Simulation. *ACM Transactions on Modeling and Computer Simulation*. Vol. 4, No. 2 (April 1994), pp. 165-90.

Lin, Ying-Dar, & Hsu, Yu-Ching. (2000). Multihop Cellular: A New Architecture for Wireless Communications. In Proceedings of IEEE INFOCOM'00 (Tel Aviv, Israel, 26-30 March 2000). 3, 1273-82.

Liu, Yajian, et al., (2006). Integrated Radio Resource Allocation for Multihop Cellular Networks with Fixed Relay Stations. *IEEE Journal on Selected Areas in Communications*. Vol. 24, No. 11 (November 2006), pp. 2137-46.

Luo, Haiyun, et al. (2003). Ucan: A Unified Cellular and Ad-Hoc Network Architecture. In Proceedings of ACM MOBICOM'03 (San Diego, CA, USA 14-19 September 2003). 1, 353-67.

Rappaport, Stephen S., & Hu, Lon-Rong, (1994). Microcellular Communication Systems with Hierarchical Macrocell Overlays: Traffic Performance Models and Analysis. *Proceedings of The IEEE*. Vol. 82, No. 9 (September 1994), pp. 1383-97.

Wu, Hongyi, et al. (2004). Managed Mobility: A Novel Concept in Integrated Wireless Systems. In Proceedings of IEEE MASS'04 (Fort Lauderdale, FL, 24-27 October 2004). 1, 537-39.

---, (2001). Integrated Cellular and Ad Hoc Relaying Systems: Icar. *IEEE Journal on Selected Areas in Communications*. Vol. 19, No. 10 (October 2001), pp. 2105-15.

Yeung, Kwan L., & Nanda, S., (1996). Channel Management in Microcell/Macrocell Cellular Radio Systems. *IEEE Transactions on Vehicular Technology*. Vol. 45, No. 4 (November 1996), pp. 601-12.

Yu, Jane Yang, & Chong, P. H. J., (2005). A Survey of Clustering Schemes for Mobile Ad Hoc Networks. *IEEE Communications Survey & Tutorials*. Vol. 7, No. 1 (First Quarter 2005), pp. 32-48.

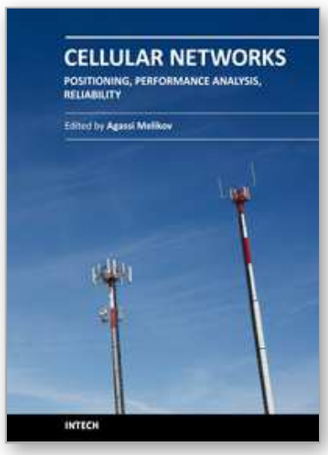

Cellular Networks - Positioning, Performance Analysis, Reliability
Edited by Dr. Agassi Melikov

ISBN 978-953-307-246-3
Hard cover, 404 pages
Publisher InTech
Published online 26, April, 2011
Published in print edition April, 2011

Wireless cellular networks are an integral part of modern telecommunication systems. Today it is hard to imagine our life without the use of such networks. Nevertheless, the development, implementation and operation of these networks require engineers and scientists to address a number of interrelated problems. Among them are the problem of choosing the proper geometric shape and dimensions of cells based on geographical location, finding the optimal location of cell base station, selection the scheme dividing the total net bandwidth between its cells, organization of the handover of a call between cells, information security and network reliability, and many others. The book focuses on three types of problems from the above list - Positioning, Performance Analysis and Reliability. It contains three sections. The Section 1 is devoted to problems of Positioning and contains five chapters. The Section 2 contains eight Chapters which are devoted to quality of service (QoS) metrics analysis of wireless cellular networks. The Section 3 contains two Chapters and deal with reliability issues of wireless cellular networks. The book will be useful to researches in academia and industry and also to post-gradute students in telecommunication specialitiies.

InTech Europe
University Campus STeP Ri
Slavka Krautzeka 83/A
51000 Rijeka, Croatia
Phone: +385 (51) 770 447
Fax: +385 (51) 686 166
www.intechopen.com

InTech China
Unit 405, Office Block, Hotel Equatorial Shanghai
No.65, Yan An Road (West), Shanghai, 200040, China
中国上海市延安西路65号上海国际贵都大饭店办公楼405单元
Phone: +86-21-62489820
Fax: +86-21-62489821

IntechOpen